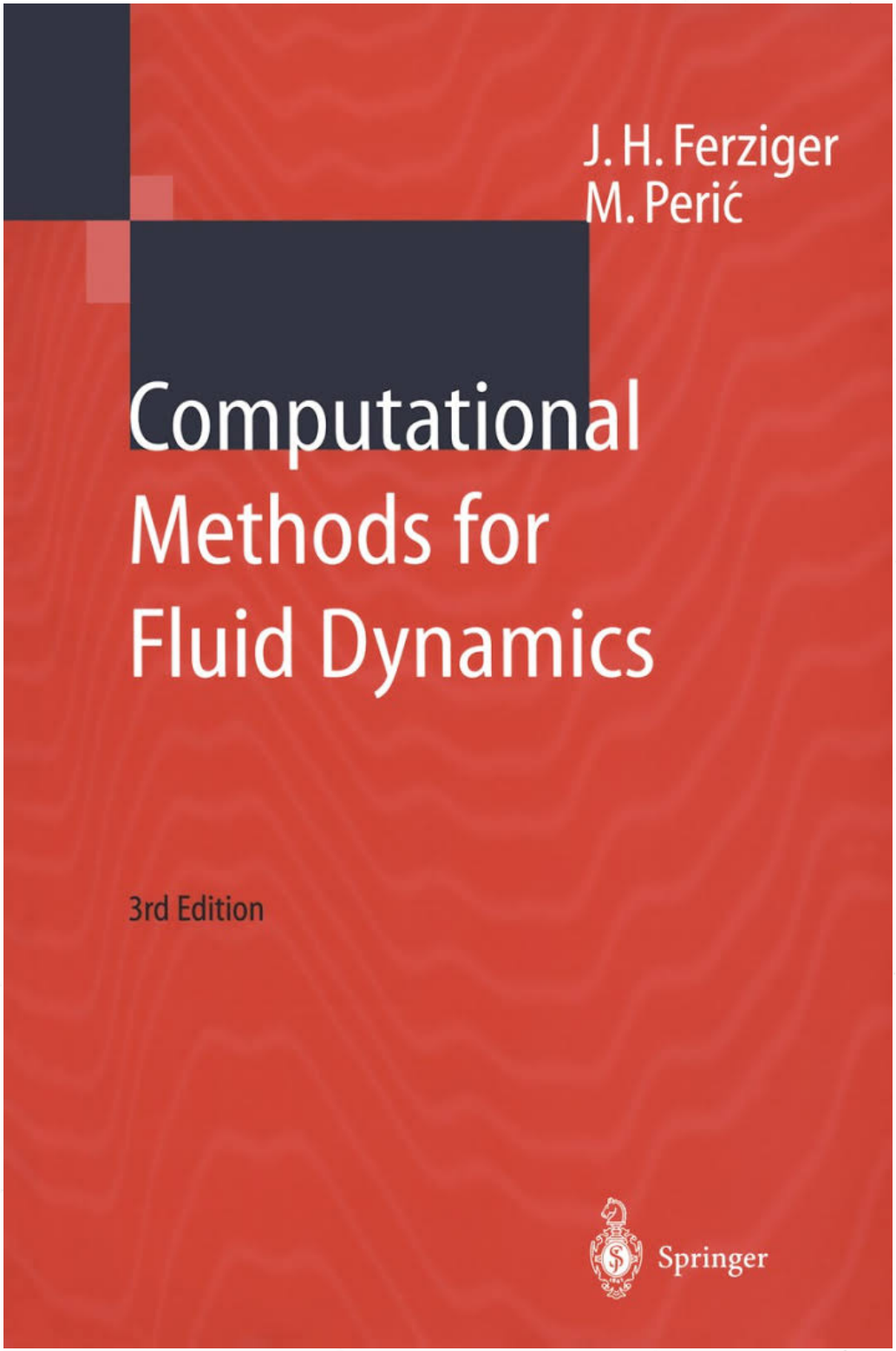

9. Turbulent Flows

9.1 Introduction

Most flows encountered in engineering practice are turbulent; they are characterized by the following properties:

- Turbulent flows are highly unsteady. A plot of the velocity as a function of time would appear random to an observer unfamiliar with these flows. The word 'chaotic' could be used but it has been given another definition in recent years.
- They are three-dimensional. The time-averaged velocity may be a function of only two coordinates, but the instantaneous field appears essentially random.
- They contain a great deal of vorticity. Stretching of vortices is one of the principal mechanisms by which the intensity of the turbulence is increased.
- Turbulence increases the rate at which conserved quantities are stirred. That is, parcels of fluid with differing concentrations of the conserved properties are brought into contact. The actual *mixing* is accomplished by diffusion. Nonetheless, this behavior is often called *diffusive*.
- By increasing the mixing of momentum, turbulence brings fluids of differing momentum content into contact. The reduction of the velocity gradients produced by the action of viscosity reduces the kinetic energy of the flow; in other words, it is *dissipative*. The lost energy is irreversibly converted into internal energy of the fluid.
- It has been shown in recent years that turbulent flows contain *coherent structures* – repeatable and essentially deterministic events that are responsible for a large part of the mixing. However, the random part of turbulent flows causes these events to differ from each other in size, strength, and time interval between occurrences, making study of them very difficult.

These properties are important. The effects produced by turbulence may or may not be desirable. Intense mixing may be useful when chemical mixing or heat transfer are needed. On the other hand, increased mixing of momentum results in increased frictional forces, so the power required to pump the fluid or the drag force on a vehicle is increased. The engineer needs to be able to understand and predict these effects in order to achieve a good design. In some cases, it is possible to control the turbulence, at least in part.

In the past, the primary approach to studying turbulent flows has been experimental. Overall parameters such as the time-averaged drag or heat transfer may be relatively easy to measure but as the required level of detail increases, so does the difficulty of making measurements. To optimize a design, it is often necessary to understand the source of the problem; this requires detailed measurements that are costly and time-consuming. Some types of measurements, for example, the fluctuating pressure within a flow, are almost impossible to make at the present time. Others cannot be made with the required precision. As a result, numerical methods have an important role to play.

Before proceeding, it is useful to introduce a classification scheme for methods of predicting turbulent flows. According to Bardina et al. (1980) there are six categories, each of which can be divided in sub-categories.

- The first involves the use of *correlations* such as the friction factor as a function of the Reynolds number or the Nusselt number of heat transfer as a function of the Reynolds and Prandtl numbers. This method, which is usually taught in introductory courses, is very useful but is limited to simple types of flows. As its use does not require the use of a computer, we shall say no more about it here.
- The second uses *integral equations* which can be derived from the equations of motion by integrating over one or more coordinates. Usually this reduces the problem to one or more ordinary differential equations which are easily solved. The methods applied to these equations are those for ordinary differential equations which are discussed in Chap. 6.
- The third is based on equations obtained by averaging the equations of motion over time (if the flow is statistically steady), over a coordinate in which the mean flow does not vary, or over an ensemble of realizations (an imagined set of flows in which all controllable factors are kept fixed). This approach is called *one-point closure* and leads to a set of partial differential equations called the Reynolds averaged Navier-Stokes (or RANS) equations. As we shall see later, these equations do not form a closed set so this method requires the introduction of approximations (*turbulence models*). The problems associated with the numerical solution of equations containing turbulence models are discussed later in this chapter.
- The fourth set of methods are called *two-point closures* and use equations for the correlation of the velocity components at two distinct points or, more often, the Fourier transform of these equations. As these methods are rarely used except for homogeneous turbulence, we shall not consider them further.
- The fifth is *large eddy simulation (LES)* and solves for the largest scale motions of the flow while modeling only the small scale motions. It can be regarded as a kind of compromise between one point methods (see above) and direct numerical simulation (see below).

- Finally, there is *direct numerical simulation (DNS)* in which the Navier-Stokes equations are solved for all of the motions in a turbulent flow.

As one progresses down this list, more and more of the turbulent motions are computed and fewer are approximated. This makes the methods close to the bottom more exact but the computation time is increased considerably.

All of the methods described in this chapter require the solution of some form of the conservation equations for mass, momentum, energy, or chemical species. The major difficulty is that, in turbulent flows, there is a much wider range of length and time scales than in laminar flows. So, even though they are similar to the laminar flow equations, the equations for turbulent flows are usually much more difficult and expensive to solve.

9.2 Direct Numerical Simulation (DNS)

The most exact approach to turbulence simulation is to solve the Navier-Stokes equations without averaging or approximation other than the necessary numerical discretizations whose errors can be estimated and controlled. It is also the simplest approach from the conceptual point of view. In such simulations, all of the motions contained in the flow are resolved. The result is equivalent to a single realization of a flow or a short-duration laboratory experiment; as noted above, this approach is called direct numerical simulation (DNS).

In a direct numerical simulation, the domain on which the computation is performed must be at least as large as the largest turbulent eddy. A useful measure of this scale is the integral scale (L) of the turbulence; the latter is essentially the distance over which the fluctuating component of the velocity remains correlated. Each linear dimension of the domain must be at least as large as a few times the integral scale. A valid simulation must also capture all of the kinetic energy dissipation. This occurs on the smallest scales, the ones on which viscosity is active, so the size of the grid must be no larger than a viscously determined scale, called the Kolmogoroff scale, η. For homogeneous turbulence, the simplest type of turbulence, there is no reason to use anything other than a uniform grid. In this case, the number of grid points in each direction must be at least L/η; it can be shown (Tennekes and Lumley, 1976) that this ratio is proportional to $\mathrm{Re}_L^{3/4}$. Here Re_L is a Reynolds number based on the magnitude of the velocity fluctuations and the integral scale; this parameter is typically about 0.01 times the macroscopic Reynolds number engineers use to describe a flow. Since this number of points must be employed in each of the three coordinate directions, and the time step is related to the grid size, the cost of a simulation typically scales as Re_L^3.

Since the number of grid points in a computation is limited by the processing speed and memory of the machine on which it is carried out, direct

numerical simulation is possible only at low Reynolds numbers. On present machines, it is possible to make direct numerical simulations of homogeneous flows at turbulent Reynolds numbers up to about 200. As noted in the preceding paragraph, this corresponds to overall flow Reynolds numbers about two orders of magnitude larger and allows DNS to reach the low end of the range of Reynolds numbers of engineering interest, making it a useful method. For further details about DNS, see Leonard (1995).

The results of a DNS contain very detailed information about the flow. This can be very useful but, on the one hand, it is far more information than any engineer needs and, on the other, DNS is too expensive to be employed very often. To what uses can DNS be put? We can obtain detailed information about the velocity, pressure, and any other variable of interest at a large number of grid points. These results may be regarded as the equivalent of experimental data and can be used to produce statistical information or to create a 'numerical flow visualization'. From the latter, one can learn a great deal about whatever coherent structures may exist in the flow. This wealth of information can then be used to develop a qualitative understanding of the physics of the flow or to construct a quantitative model which will allow other, similar, flows to be computed.

Some examples of the uses to which DNS has been put are:

- Understanding the mechanisms of turbulence production, energy transfer, and dissipation in turbulent flows;
- Simulation of the production of aerodynamic noise;
- Understanding the effects of compressibility on turbulence;
- Understanding the interaction of combustion and turbulence;
- Controlling and reducing drag on a solid surface.

The increasing speed of computers has made it possible to carry out DNS of simple flows at very low Reynolds numbers on workstations. By simple flows, we mean any homogeneous turbulent flow (there are many), channel flow, and a few others. On large parallel computers, it is possible to do DNS with 512^3 ($\sim 1.35 \times 10^8$) or more grid points; about one minute of computer time is required per time step on an Intel Delta parallel computer. This means that a complete simulation requires no less than ten and sometimes many hundred hours. We expect that increasingly complex flows will be simulated.

A wide variety of numerical methods can be employed in direct numerical simulation and large eddy simulation. Almost any method found in this book can be used. Because these methods have been described in earlier chapters, we shall not give a lot of detail here. Instead, a few issues peculiar to DNS and LES will be discussed.

The most important requirements on numerical methods for DNS or LES arise from the need to produce an accurate realization of a flow that contains a wide range of length scales. Because a time history is required, techniques designed for steady flows cannot be used without considerable modification.

Accuracy requires the time step to be small and, of course, the time-advance method must be stable for the time step selected. This condition is usually met by explicit methods so there is no reason to incur the extra expense associated with implicit methods; most simulations have used explicit time advance methods. Notable exceptions occur close to walls where very fine grids must be used to resolve the flow structures. Here, instability may arise from the viscous terms involving derivatives normal to the wall and these terms may need to be treated implicitly. In complex geometries, it may be necessary to treat still more terms implicitly. The time advance methods most commonly used in DNS and LES are of second to fourth order accuracy; Runge-Kutta methods have been used most commonly but others, such as Adams-Bashforth, leapfrog, and Crank-Nicolson (for the terms that must be treated implicitly) have found application.

However, most of these methods require storage of data at a number of time steps (including intermediate time steps) and, as the amount of data contained in a single velocity field is large, it is important to minimize the storage requirements. Thus, Leonard and Wray (1982) presented a third order Runge-Kutta method which requires less storage than the standard Runge-Kutta method of that accuracy.

A further issue of importance in DNS is the need to handle a wide range of length scales; this requires a change from the usual way of thinking about discretization methods. The most common descriptor of the accuracy of a spatial discretization method is its order, a number that describes the rate at which the discretization error decreases when the grid size is reduced. To see why this is not an appropriate indicator of accuracy in DNS or LES, it is useful to think in terms of the Fourier decomposition of the velocity field. We saw earlier (Sect. 3.8) that, on a uniform grid, the velocity field can be represented in terms of its Fourier components:

$$u(x) = \sum \tilde{u}(k)\, \mathrm{e}^{\mathrm{i}kx} \tag{9.1}$$

The highest wavenumber k that can be resolved on a grid of size Δx is $\pi/\Delta x$, so we consider only $0 < k < \pi/\Delta x$. The exact derivative of $\mathrm{e}^{\mathrm{i}kx}$ is, of course, $\mathrm{i}k\mathrm{e}^{\mathrm{i}kx}$. A discrete approximation replaces this by $\mathrm{i}k_{\mathrm{eff}}\mathrm{e}^{\mathrm{i}kx}$ where k_{eff} is the effective wavenumber defined in Sect. 3.8. The plot of k_{eff} given in Fig. 3.4 shows that central differences are accurate only for $k < \pi/2\Delta x$, the first half of the wavenumber range of interest.

The problem is that a turbulence spectrum (the distribution of its energy over wavenumber) covers a significant part of the wavenumber range $\{0, \pi/\Delta x\}$. The order of the method is no longer a good definition of accuracy. A better measure of error is:

$$\epsilon_1 = \frac{\int (k - k_{\text{eff}}) E(k)\, \mathrm{d}k}{\int k E(k)\, \mathrm{d}k}\,, \tag{9.2}$$

where $E(k)$ is the energy spectrum of the turbulence and, in one dimension is $\hat{u}(k)\hat{u}^*(k)/2$, where the asterisk indicates complex conjugation. Similar expressions can be given for the second derivative. Using the measure (9.2), Cain et al. (1981) found that, for a spectrum typical of isotropic turbulence, a fourth order method had half the error of a second order method, much more than one would anticipate.

The methods and step sizes in time and space need to be related. The errors made in the spatial and temporal discretizations should be as nearly equal as possible i.e. they should be balanced. This is not possible point-by-point and for every time step but, if this condition is not satisfied in an average sense, one is using too fine a step in one of the independent variables and the simulation could be made at lower cost with little loss of accuracy.

Accuracy is difficult to measure in DNS and LES. The reason is inherent in the nature of turbulent flows. A small change in the initial state of a turbulent flow is amplified exponentially in time and, after a relatively short time, the perturbed flow hardly resembles the original one. So, direct comparison of two solutions with the goal of determining the error is not possible. Instead, one can repeat the simulation with a different grid (which should differ considerably from the original one) and statistical properties of the two solutions can be compared. From the difference, an estimate of the error can be found. A simpler possibility, which has been used by most people who compute simple turbulent flows, is to look at the spectrum of the turbulence. If the energy in the smallest scales is sufficiently smaller than that at the peak in the energy spectrum, it is probably safe to assume that the flow has been well resolved.

The accuracy requirement makes use of spectral methods common in DNS and LES. These methods were described earlier, in Sect. 3.8. In essence, they use Fourier series as a means of obtaining derivatives. The use of Fourier transforms is feasible only because the fast Fourier transform algorithm (Cooley and Tukey, 1965) reduces this cost to $n \log_2 n$ operations. This algorithm is available only for equi-spaced points and a few other special cases. A number of specialized methods of this kind have been developed for solving the Navier-Stokes equations; the reader interested in more details of spectral methods is referred to the book by Canuto et al. (1987).

We briefly mention one special method. Rather than directly approximating the Navier-Stokes equations, one could multiply them by a sequence of 'test functions' and integrate over the entire domain; this is essentially the basis of finite element methods. Functions which satisfy this form of the equations are known as 'weak solutions'. One can represent the solution of the Navier-Stokes equations in the form of a series of vector functions, each of

which has zero divergence. This choice removes the pressure from the integral form of the equations, thereby reducing the number of dependent variables that need to be computed and stored. The set of dependent variables can be further reduced by noting that, if a function has zero divergence, its third component can be computed from the other two. The result is that only two sets of dependent variables need to be computed, reducing the memory requirements by half. As these methods are quite specialized and their development requires considerable space, they are not given in detail here; the interested reader is referred to the paper by Leonard (1974).

Another difficulty in DNS is that of generating initial and boundary conditions. The former must contain all the details of the initial three dimensional velocity field; the inflow conditions must contain the complete velocity field on a plane of a turbulent flow at each time step. Since the effects of initial and boundary conditions may be remembered by the flow for a considerable time, they can have a significant effect on the results. The details are flow dependent and so are not described here but we give a brief description of the idea. For flows which do not vary (in the statistical sense) in a given direction, one can often use periodic boundary conditions; these are easy to use, fit especially well with spectral methods and provide conditions which are as realistic as possible. When periodic boundary conditions cannot be used, the best initial and inflow conditions are obtained from the results of other simulations. For example, if one requires the flow at the inlet to a curved channel, a good source might be a simulation of flow in a plane channel. In the process of simulating plane channel flow, the velocity components on a plane normal to the main flow direction are recorded; they provide the inflow to the curved channel. Similarly, the initial conditions for strained homogeneous turbulence are usually adopted from a simulation of isotropic turbulence.

Outflow boundaries are less difficult to handle. One possibility is to use extrapolation conditions which require the derivatives of all quantities in the direction normal to the boundary be zero:

$$\frac{\partial \phi}{\partial n} = 0\,, \tag{9.3}$$

where ϕ is any of the dependent variables. This condition is often used in steady flows but is not satisfactory in unsteady flows. For the latter, it is better to replace this condition by an unsteady convective condition. A number of such conditions have been tried but the one that appears to work best is also the simplest:

$$\frac{\partial \phi}{\partial t} - U \frac{\partial \phi}{\partial n} = 0\,, \tag{9.4}$$

where U is a velocity that is independent of location on the outflow surface and is chosen so that overall conservation is maintained i.e. it is the velocity required to make the outflow mass flux equal to the incoming mass flux.

This condition appears to avoid the problem caused by pressure waves being reflected off the outflow boundary back to the interior of the domain.

On solid walls, no slip boundary conditions, which have been described in Chaps. 7 and 8 may be used. One must bear in mind that at boundaries of this type the turbulence tends to develop small but very important structures ('streaks') that require very fine grids (especially in the direction normal to both the wall and the principal flow direction.

Symmetry boundary conditions, which are often used in RANS computations to reduce the size of the domain are usually not applicable in DNS or LES because, although the mean flow may be symmetric about some particular plane, the instantaneous flow is not and important physical effects may be removed by application of conditions of this type. Symmetry conditions have, however, been used to represent free surfaces.

Despite all attempts to make the initial and boundary conditions as realistic as possible, a simulation must be run for some time before the flow develops all of the correct characteristics of the physical flow. This situation reflects the physics of turbulent flows so there is little one can do to speed up the process; one possibility is mentioned below. The time scale for the development of simple flows is the so-called eddy-turnover time which is the ratio of the integral scale of the turbulence to a characteristic velocity associated with the turbulence. In these flows, this time scale can be related to a time scale characteristic of the flow as a whole i.e. a mean flow time scale, but in separated flows, there are regions that communicate slowly with the remainder of the flow and the development process can be very slow.

The best way to ascertain that flow development is complete is to monitor some quantity, preferably one that is sensitive to the parts of the flow that are slow to develop; the choice depends on the flow being simulated. As an example, one might measure a spatial average of the skin friction in the recirculating region of a separated flow as a function of time. Initially, there is usually a systematic increase or decrease of the monitored quantity; when the flow is developed, the value will show statistical fluctuations with time. After the flow is developed, statistical average results (for example, for the mean velocity or its fluctuations) may be obtained by averaging over time and/or any statistically homogeneous coordinate in the flow. In so doing it is important to remember that, because turbulence is not purely random, the sample size is not the same as the number of points used in the averaging process. A conservative estimate is that each volume of diameter equal to the integral scale (and each time period equal to the integral time scale) represents only a single sample.

The development process can be sped up by using a coarser grid initially. When the flow is developed on that grid, the finer grid can be introduced. If this is done, some waiting is still necessary for the flow to develop on the fine grid but it may be less than the time that would have been required had the fine gird been used throughout the simulation.

9.2.1 Example: Spatial Decay of Grid Turbulence

As an illustrative example of what DNS can accomplish, we shall take a deceptively simple flow, the flow created by an oscillating grid in a large body of quiescent fluid. The grid creates turbulence which decreases in intensity with distance from the grid. This process is called *turbulent diffusion* and its prediction is important in many flows. It is also surprisingly difficult to model. Briggs et al. (1995) made simulations of these flows and obtained good agreement with the experimentally determined rate of decay of the turbulence with distance from the grid. The energy decays approximately as x^{-3}; determination of the exponent of decay is difficult both experimentally and computationally because the rapid decay does not provide a large enough region to compute its value accurately.

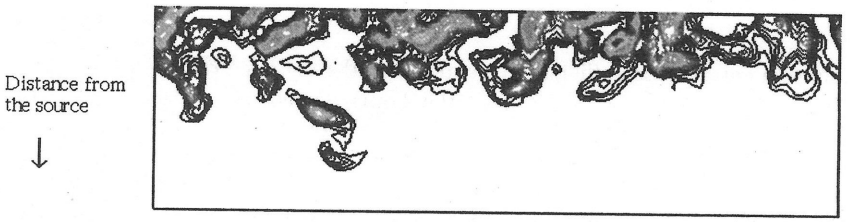

Fig. 9.1. Contours of the kinetic energy on one plane in the flow created by an oscillating grid in a large body of quiescent fluid; from Briggs et al. (1995)

Using simulated visualizations of the flow, they were able to show that the dominant mechanism of turbulent diffusion in this flow is the movement of energetic parcels of fluid through the undisturbed fluid which seems simple but is contrary to earlier proposals. Figure 9.1 shows the contours of the kinetic energy on one plane in this flow. One sees that the large energetic regions are of the same size throughout the flow but there are fewer of them far from the grid. The reasons are that those that propagate parallel to the grid do not move very far in the direction normal to the grid and that the smaller 'blobs' of energetic fluid are quickly destroyed by the action of viscous diffusion.

The results were used to test turbulence models. A typical example of such a test is shown in Fig. 9.2 in which the profile to the flux of turbulent kinetic energy is given and compared with the predictions of some commonly used turbulence models. It is clear that the models do not work very well even in a flow as simple as this one.

The simulation used a code that was originally designed for the simulation of homogeneous turbulence (Rogallo, 1981). Periodic boundary conditions are applied in all three directions; this implies that there is actually a periodic array of grids but this causes no problem so long as the distance between

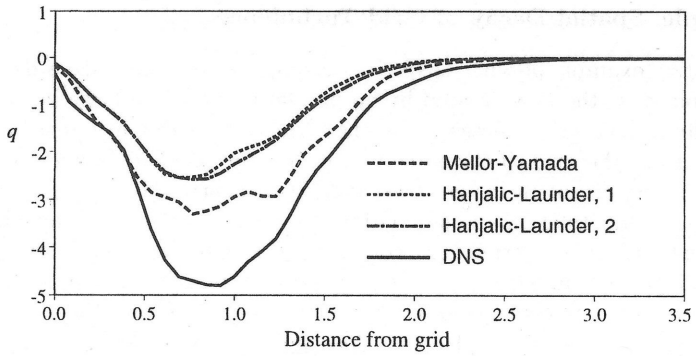

Fig. 9.2. The profile of the flux of turbulent kinetic energy, q, compared with the predictions of some commonly used turbulence models (Mellor and Yamada, 19??; Hanjalić and Launder, 1976 and 1980); from Briggs et al. (1995)

subsequent grids is sufficiently greater than the distance required for the turbulence to decay. The code uses the Fourier spectral method in all three spatial directions and a third order Runge-Kutta method in time.

These results illustrate some important features of DNS. It is possible to compute statistical quantities that are useful is assessing models and comparing with experiments and visualizations of the same flow. This is rarely possible in the laboratory. The combination allows one to develop an understanding of the physics of the flow that can be very useful in modeling and control of turbulence.

In direct numerical simulations, one can control the external variables in a manner that is difficult or impossible to implement in the laboratory. There are several cases in which the results of DNS disagreed with those of experiments and in which the former turned out to be more nearly correct. One example is the distribution of turbulent statistics near a wall; the results of Kim et al. (1987) proved to be more accurate than the experiments when both were repeated with more care. Another example was provided by Bardina et al. (1980) which explained some apparently anomalous results in an experiment on the effects of rotation on isotropic turbulence.

DNS makes it possible to investigate certain effects much more accurately than would be otherwise possible. It is also possible to try methods of control that cannot be realized experimentally. The point of doing so is to provide insight into the physics of the flow and thus to indicate possibilities that may be realizable (and to point the direction toward realizable approaches). An example is the study of drag reduction and control on a flat plate conducted by Choi et al. (1994). They showed that, by using controlled blowing and suction through the wall (or pulsating wall surface), the turbulent drag of a flat plate could be reduced by 30%.

9.3 Large Eddy Simulation (LES)

As we have seen, turbulent flows contain a wide range of length and time scales; the range of eddy sizes that might be found in a flow is shown schematically on the left hand side of Fig. 9.3. The right side of this figure shows a typical velocity component at a point in the flow; the range of scales is obvious.

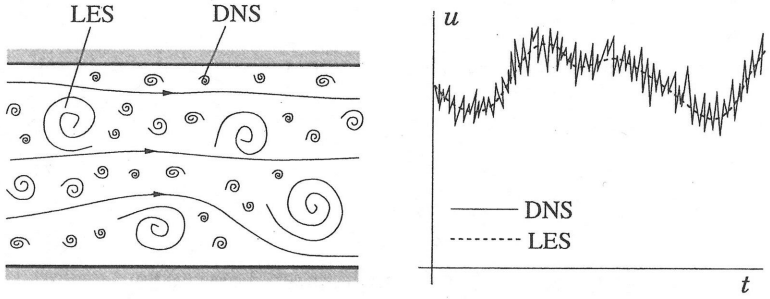

Fig. 9.3. Schematic representation of turbulent motion (left) and the time dependence of a velocity component at a point (right)

The large scale motions are generally much more energetic than the small scale ones and their size and strength make them by far the most effective transporters of the conserved properties. The small scales are usually much weaker, and provide little transport of these properties. A simulation which treats the large eddies more exactly than the small ones may make sense; large eddy simulation is such an approach. Large eddy simulations are three dimensional, time dependent and expensive but much less costly than a DNS of the same flow. In general, because it is more accurate, DNS is to be preferred whenever it is feasible. LES is the preferred method for flows in which the Reynolds number is too high or the geometry is too complex for the application of DNS.

It is essential to define the quantities to be computed precisely. We need a velocity field that contains only the large scale components of the total field. This is best done by filtering (Leonard, 1974); the large or resolved scale field, the one to be simulated, is essentially a local average of the complete field. We shall use one-dimensional notation; the generalization to three dimensions is straightforward. The filtered velocity is defined by:

$$\overline{u}_i(x) = \int G(x,x')\, u_i(x')\, \mathrm{d}x' \,, \tag{9.5}$$

where $G(x,x')$, the filter kernel, is a localized function. Filter kernels which have been applied in LES include a Gaussian, a box filter (a simple local average) and a cutoff, a filter which eliminates all Fourier coefficients belonging

to wavenumbers above a cutoff. Every filter has associated with it, a length scale, Δ. In a rough sense, eddies of size large than Δ are large eddies while those smaller than Δ are small eddies, the ones that will need to be modeled.

When the Navier-Stokes equations for constant density (incompressible flow) are filtered, one obtains a set of equations very similar in form to the RANS equations:

$$\frac{\partial(\rho\overline{u}_i)}{\partial t} + \frac{\partial(\rho\overline{u_i u_j})}{\partial x_j} = -\frac{\partial \overline{p}}{\partial x_i} + \frac{\partial}{\partial x_j}\left[\mu\left(\frac{\partial \overline{u}_i}{\partial x_j} + \frac{\partial \overline{u}_j}{\partial x_i}\right)\right] . \tag{9.6}$$

Since the continuity equation is linear, filtering does not change it significantly:

$$\frac{\partial(\rho\overline{u}_i)}{\partial x_i} = 0 . \tag{9.7}$$

It is important to note that since:

$$\overline{u_i u_j} \neq \overline{u}_i \overline{u}_j , \tag{9.8}$$

and the quantity on the left side of the inequality is not easily computed, a modeling approximation for the difference between the two sides of this inequality,

$$\tau^s_{ij} = -\rho(\overline{u_i u_j} - \overline{u}_i \overline{u}_j) \tag{9.9}$$

must be introduced. In the context of LES, τ^s_{ij} is called the *subgrid scale Reynolds stress*. The name 'stress' stems from the way in which it is treated rather than its physical nature. It is in fact the large scale momentum flux caused by the action of the small or unresolved scales. The name 'subgrid scale' is also somewhat of a misnomer. The width of the filter, Δ, need not have anything to do with the grid size, h, other than the obvious condition that $\Delta > h$. Some authors (including many of the early ones) do make such a connection and the nomenclature they introduced has stuck. The models used to approximate the SGS Reynolds stress (9.9) are called *subgrid scale (SGS) models.*

The subgrid scale Reynolds stress is a local average of the small scale field so models for it should be based on the local velocity field or, perhaps, on the past history of the local fluid. The latter can be accomplished by using a model that solves partial differential equations to obtain the parameters needed to determine the SGS Reynolds stress.

9.3.1 Smagorinsky and Related Models

The most commonly used subgrid scale model is one proposed by Smagorinsky (1963). It is an eddy viscosity model which is based on the notion that the effects of the SGS Reynolds stress are increased transport and dissipation. As these are effects of viscosity in laminar flows, it seems reasonable to assume that a reasonable model might be:

$$\tau^s_{ij} - \frac{1}{3}\tau^s_{kk}\delta_{ij} = \mu_t\left(\frac{\partial \overline{u}_i}{\partial x_j} + \frac{\partial \overline{u}_j}{\partial x_i}\right) = 2\mu_t \overline{S}_{ij} , \tag{9.10}$$

where μ_t is the eddy viscosity. This model can be derived in a number of ways including heuristic methods, for example, by equating production and dissipation of subgrid scale turbulent kinetic energy, or via turbulence theories.

The form of the subgrid scale eddy viscosity can be derived by dimensional arguments and is:

$$\mu_t = C_S^2 \rho \Delta^2 |\overline{S}| , \tag{9.11}$$

where C_S is the model parameter, Δ is the filter length scale, $|\overline{S}| = (\overline{S}_{ij}\overline{S}_{ij})^{1/2}$. This result can also be derived in a number of ways. Theories provide estimates of the constant. Most of these are valid only for isotropic turbulence but they agree that $C_S \approx 0.2$. However, C_S is not constant and may be a function of Reynolds number and other non-dimensional parameters and may be different in different flows.

The Smagorinsky model, although relatively successful, is not without problems. For example, to simulate channel flow, several modifications are required. The value of the parameter C_S in the bulk of the flow has to be reduced from 0.2 to approximately 0.065, which reduces the eddy viscosity by almost an order of magnitude. In regions close to surfaces, the value has to be reduced even further. One successful recipe is the van Driest damping that has long been used to reduce the near-wall eddy viscosity in RANS models:

$$C_S = C_{S0}\left(1 - e^{-n^+/A^+}\right)^2 , \tag{9.12}$$

where n^+ is the distance from the wall in viscous wall units ($n^+ = nu_\tau/\nu$, where u_τ is the shear velocity, $u_\tau = \sqrt{\tau_w/\rho}$, and τ_w is the shear stress at the wall) and A^+ is a constant usually taken to be approximately 25. Although this modification produces the desired results, it is difficult to justify in the context of LES. The SGS model should depend solely on the local properties of the flow and it is difficult to see how the distance from the wall qualifies in this regard.

The purpose of the van Driest damping is to reduce the subgrid scale eddy viscosity near the wall; $\mu_t \sim n^3$ in this region and models should respect this property. An alternative is a subgrid scale model which reduces the eddy viscosity when the subgrid scale Reynolds number, $|\overline{S}|\Delta^2/\nu$, becomes small. Models of this kind were suggested by McMillan and Ferziger (1980) and by Yakhot and Orszag (1986); the latter used renormalization group theory to derive their model.

A further problem is that, near a wall, the flow structure is very anisotropic. Regions of low and high speed fluid (streaks) are created; they are approximately 1000 viscous units long and 30-50 viscous units wide in both the spanwise and normal directions. Resolving the streaks requires a highly anisotropic

grid and the choice of length scale, Δ, to use in the SGS model is not obvious. The usual choice is $(\Delta_1\Delta_2\Delta_3)^{1/3}$ but $(\Delta_1^2+\Delta_2^2+\Delta_3^2)^{1/2}$ is possible and others are easily constructed; here Δ_i it the width associated with the filter in the ith coordinate direction. It is possible that, with a proper choice of length scale, the damping (9.12) would become unnecessary. A fuller discussion of this issue can be found in Piomelli et al. (1989).

In a stably stratified fluid, it is necessary to reduce the Smagorinsky parameter. This situation is common in geophysical flows; the practice is to make the parameter a function of Richardson number, a non-dimensional parameter that represents the relative importance of stratification and shear. Similar effects occur in flows in which rotation and/or curvature play significant roles.

Thus there are many difficulties with the Smagorinsky model. If we wish to simulate more complex and/or higher Reynolds number flows, it may be important to have a more accurate model. Indeed, detailed tests based on results derived from DNS data, show that the Smagorinsky model is quite poor.

The small scales of a simulation are similar in many ways to the still smaller scales that are treated via the model. This idea leads to an alternative subgrid scale model, the *scale similarity model* (Bardina et al., 1980). The principal argument is that the important interactions between the resolved and unresolved scales involve the smallest eddies of the former and the largest eddies of the latter i.e., eddies that are a little larger or a little smaller than the length scale, Δ, associated with the filter. This leads to the following model:

$$\tau_{ij}^{s} = -\rho(\overline{u}_i\overline{u}_j - \overline{\overline{u}}_i\overline{\overline{u}}_j) \,, \tag{9.13}$$

where the double overline indicates a quantity that has been filtered twice. The constant is required to be unity in order to satisfy Galilean invariance. This model correlates very well with the actual SGS Reynolds stress, but hardly dissipates any energy and cannot serve as a 'stand alone' SGS model. It transfers energy from the smallest resolved scales to larger scales, which is useful. To correct for the lack of dissipation, it is necessary to combine the Smagorinsky and scale similarity models to produce a 'mixed' model. This model improves the quality of simulations. For further details, see Bardina et al. (1980).

9.3.2 Dynamic Models

The concept underlying the scale similarity model, namely that the smallest resolved scale motions and the largest subgrid scale motions are similar in structure, can be taken a step further, leading to the dynamic model or procedure (Germano et al., 1990). It assumes that one of the models described above is acceptable.

One way to understand the concept is the following. Suppose we do a large eddy simulation on a fine grid. Let us, for the sake of argument, regard the results as an exact representation of a velocity field. We can then use

the following procedure to estimate the subgrid scale model parameter. The velocity field $\overline{u}_i$ can itself be filtered (using a filter broader than the one used in the LES) to obtain a very large scale field $\overline{u}_i$; the corresponding subgrid scale field can be obtained by subtraction of the two fields. By multiplication and filtering, one can compute the subgrid scale Reynolds stress tensor. From the large scale field, one can also construct the estimate of this field that the model would produce. By comparing these two, we can test the quality of the model in a direct way and, even more importantly, compute the value of the model parameter. This can be done at every spatial point and every time step. The value of the parameter can then be applied to the subgrid scale model of the large eddy simulation itself. In this way, a kind of self-consistent subgrid scale model is produced.

The actual procedure of Germano et al. is a bit more formal than what we have just suggested but the result is the same; the model parameter can be computed, at every spatial grid point and every time step, directly from results of the LES itself. We shall not present the formal procedure here. The interested reader is referred to the original paper of Germano et al. (1990) or the review by Ferziger (1995).

This method of modeling the subgrid scale should be called a procedure rather than a model as any model can be used as a basis for it. In any case, it has been shown to produce excellent results. In particular, the dynamic procedure removes many of the difficulties described earlier:

- In shear flows, the Smagorinsky model parameter needs to be much smaller than in isotropic turbulence. The dynamic model captures this change automatically.
- The model parameter has to be reduced even further near walls. The dynamic model automatically decreases the parameter in the correct manner near the wall.
- The definition of the length scale for anisotropic grids or filters is unclear. This issue becomes moot with the dynamic model because the model compensates by changing the value of the parameter.

Although it improves considerably on the Smagorinsky model, there are problems with the dynamic procedure. The model parameter it produces is a rapidly varying function of the spatial coordinates and time so the eddy viscosity takes on large values of both signs. Although negative eddy viscosity may be considered as a way of representing energy transfer from the small scales to the large ones, a process that is called *backscatter*, if the eddy viscosity is negative over too large a spatial region or for too long a time, numerical instability may and does occur. One cure is to set any eddy viscosity $\mu_t < -\mu$, the molecular viscosity, equal to $-\mu$. Another useful alternative is to employ averaging in space or time. For details, the reader is referred to the papers cited above. These techniques produce excellent results but are not completely satisfactory; finding a more robust model for the subgrid scale is the subject of current research.

The arguments on which the dynamic model is based are not restricted to the Smagorinsky model. One could, instead, use the mixed Smagorinsky–scale-similarity model. The mixed model was used by Zang et al. (1993) and Shah and Ferziger (1995) with considerable success.

The boundary conditions and numerical methods used for LES are essentially the same as those used in DNS. The most important difference is that, when LES is applied to flows in complex geometries, some numerical methods (for example, spectral methods) become difficult to apply. In these cases, one is forced to use finite difference or finite volume methods. In principle, any of the methods described earlier in this book could be used, but it is important to bear in mind that structures that challenge the resolution of the grid may exist almost anywhere in the flow. For this reason, it is important to employ methods of the highest accuracy possible.

In LES, it is possible to use wall functions of the kind used in RANS modeling (see next section). This approach has been shown to work well for attached flows (see Piomelli et al., 1989) but it is not yet known whether this approach can be made to work for separated flows.

It is also important to note that, because LES and DNS require large amounts of computer time, the programs used to make these kinds of simulations are usually special purpose codes i.e., they are written for a specific geometry and contain many special programming elements designed to obtain the highest performance on a particular machine. This is also the reason why the discretization methods are often particular to the problem being solved.

9.3.3 Example: Flow Over a Wall-Mounted Cube

As an example of the method, we shall use the flow over a cube mounted on one wall of a channel. The geometry is shown in Fig. 9.4. For the simulation shown, which was made by Shah and Ferziger (1995), the Reynolds number based on the maximum velocity at the inflow and the cube height is 3200. The inflow is fully developed channel flow and was taken from a separate simulation of that flow, the outlet condition was the convective condition given above. Periodic boundary conditions were used in the spanwise direction and no-slip conditions at all wall surfaces.

The LES used a grid of $240 \times 128 \times 128$ control volumes with second order accuracy. The time advancement method was of the fractional step type. The convective terms were treated explicitly by a third order Runge-Kutta method in time while the viscous terms were treated implicitly. In particular, the method used for the latter was an approximate factorization of the Crank-Nicolson method. The pressure was obtained by solving a Poisson equation with the multigrid method.

Figure 9.5 gives the streamlines of the time-averaged flow in the region close to the wall; a great deal of information about the flow can be discerned from this plot. The incoming flow does not separate in the traditional sense but reaches a stagnation or saddle point (marked by A on the figure) and

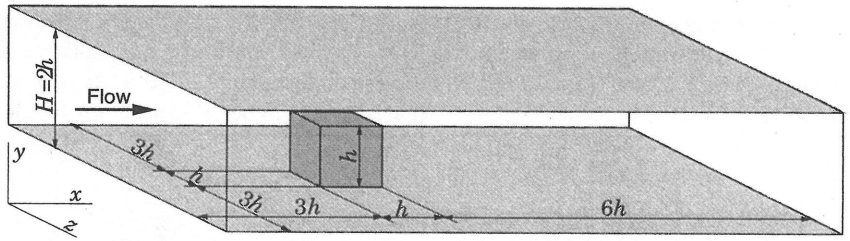

Fig. 9.4. The solution domain for the flow over a cube mounted on a channel wall; from Shah and Ferziger, (1995)

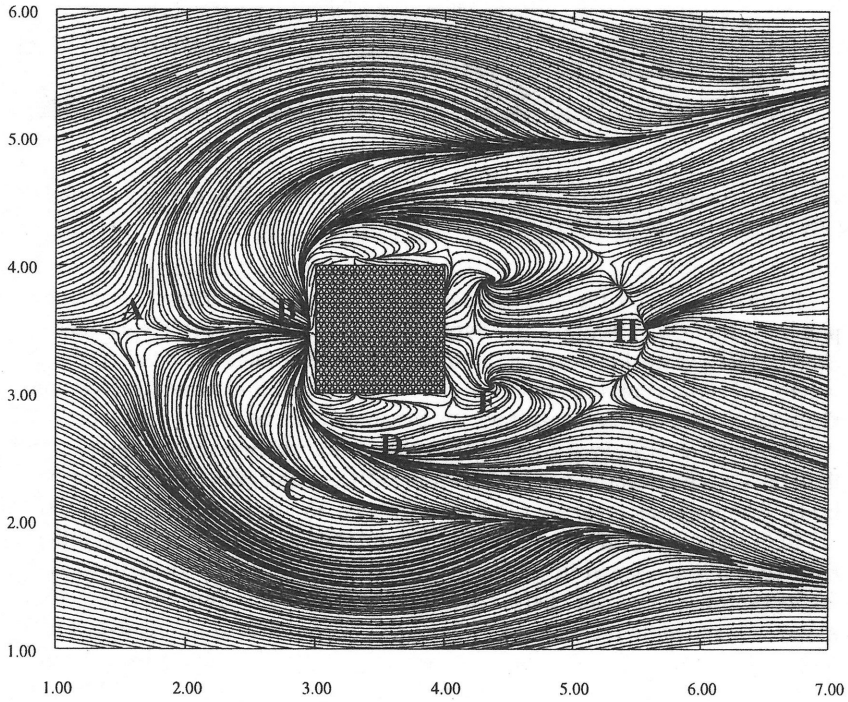

Fig. 9.5. The streamlines in the region close to the lower wall of the flow over a wall-mounted cube; from Shah and Ferziger (1995)

goes around the body. Some of the flow further above the lower wall hits the front face of the cube; about half of it flows downwards and creates the region of reversed flow in front of the body. As the flow down the front face of the cube nears the lower wall, there is a secondary separation and a reattachment line (marked by B in the figure) just ahead of the cube. To the sides of the cube, one finds a region of converging streamlines (marked as C) and another

of diverging streamlines (marked D); these are the traces of the horseshoe vortex (about which more is said below). Behind the body one finds two areas of swirling flow (marked E) which are the footprints of an arch vortex. Finally, there is a reattachment line (marked H) further downstream of the body.

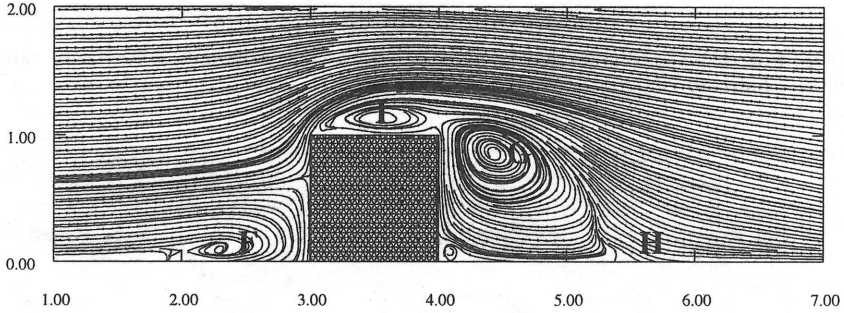

Fig. 9.6. The streamlines in the vertical center plane of the flow over a wall-mounted cube; from Shah and Ferziger (1995)

Figure 9.6 shows the streamlines of the time-averaged flow in the center plane of the flow. Many of the features described above are clearly seen including the separation zone in the upstream corner (F), the head of the arch vortex (G), the reattachment line (H), and the recirculation zone (I) above the body which does not reattach on the upper surface.

Finally, Fig. 9.7 gives a projection of the streamlines of the time-averaged flow on a plane parallel to the back face of the cube just downstream of the body. The horseshoe vortex (J) is clearly seen as are smaller corner vortices.

It is important to note that the instantaneous flow looks very different than the time averaged flow. For example, the arch vortex does not exist in an instantaneous sense; there are vortices in the flow but they are almost always asymmetric on the two sides of the cube. Indeed, the near-symmetry of Fig. 9.5 is an indication that the averaging time is (almost) long enough.

It is clear from these results that an LES (or DNS for simpler flows) provides a great deal of information about a flow. Performing such a simulation has more in common with doing an experiment than it does to the types of simulations described below.

9.4 RANS Models

Engineers are normally interested in knowing just a few quantitative properties of a turbulent flow, such as the average forces on a surface (and, perhaps, its distribution), the degree of mixing between two incoming streams of fluid,

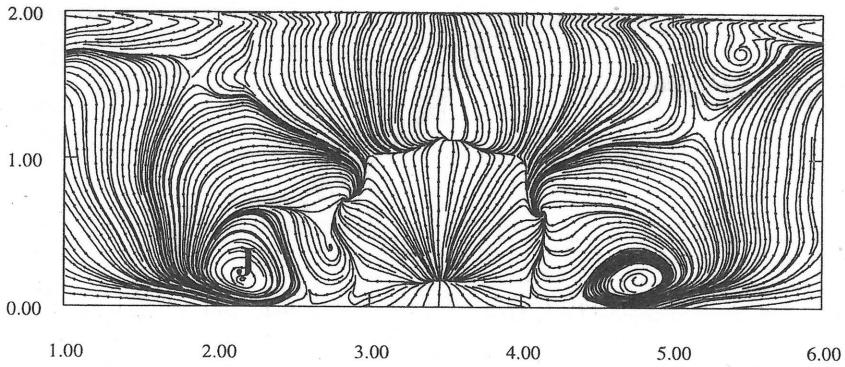

Fig. 9.7. The projection of streamlines of the flow over a wall-mounted cube onto a plane parallel to the back face, 0.1 step hight behind the cube; from Shah and Ferziger (1995)

or the amount of a substance that has reacted. Using the methods described above to compute these quantities is, to say the least, overkill. These methods should only be used as a last resort, when nothing else succeeds. In this section, we shall describe an approach that produces less information, the Reynolds-averaged method.

In Reynolds averaged approaches to turbulence, all of the unsteadiness is averaged out i.e. all unsteadiness is regarded as part of the turbulence. On averaging, the nonlinearity of the Navier-Stokes equations gives rise to terms that must be modeled. The complexity of turbulence makes it unlikely that any single model will be able to represent all turbulent flows so turbulence models should be regarded as engineering approximations rather than scientific laws.

9.4.1 Reynolds Averaged Navier-Stokes (RANS) Equations

In a statistically steady flow, every variable can be written as the sum of an average value and a fluctuation about that value:

$$\phi(x_i,t) = \overline{\phi}(x_i) + \phi'(x_i,t) \tag{9.14}$$

where

$$\overline{\phi}(x_i) = \lim_{T\to\infty} \frac{1}{T} \int_0^T \phi(x_i,t)\,\mathrm{d}t\,. \tag{9.15}$$

Here t is the time and T is the averaging interval. This interval must be large compared to the typical time scale of the fluctuations; thus, $T \to \infty$, see Fig. 9.8. If T is large enough, $\overline{\phi}$ does not depend on the time at which the averaging is started.

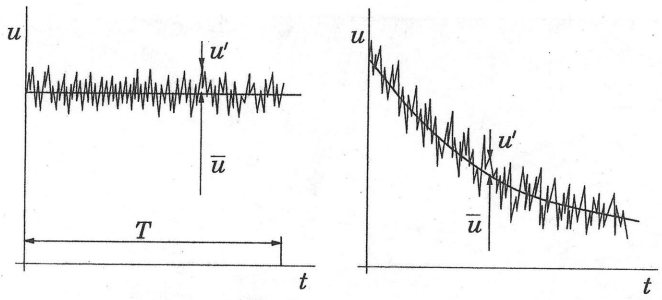

Fig. 9.8. Time averaging for a statistically steady flow (left) and ensemble averaging for an unsteady flow (right)

If the flow is unsteady, time averaging cannot be used and must be replaced by ensemble averaging, see Fig. 9.8:

$$\overline{\phi}(x_i,t) = \lim_{N\to\infty} \frac{1}{N} \sum_{n=1}^{N} \phi(x_i,t) \,, \tag{9.16}$$

where N is the number of members of the ensemble (an imagined set of flows in which all controllable variables are identical) which must be large enough to eliminate the effects of the fluctuations. This type of averaging can be applied to any flow. We use the term *Reynolds averaging* to refer to any of these averaging processes; the result of applying it to the Navier-Stokes equations is the Reynolds-averaged Navier-Stokes (RANS) equations.

From Eq. (9.15), it follows that $\overline{\phi'} = 0$. Thus, averaging any linear term in the conservation equations simply gives the identical term for the averaged quantity. From a quadratic nonlinear term we get two terms, the product of the average and a covariance:

$$\overline{u_i\phi} = \overline{(\overline{u}_i + u_i')(\overline{\phi} + \phi')} = \overline{u}_i\overline{\phi} + \overline{u_i'\phi'} \,. \tag{9.17}$$

The last term is zero only if the two quantities are uncorrelated; this is rarely the case and, as a result, the conservation equations contain terms such as $\rho\overline{u_i'u_j'}$, called the *Reynolds stresses*, $\rho\overline{u_i'\phi'}$, known as the *turbulent scalar flux*, among others. These cannot be represented uniquely in terms of the mean quantities.

The averaged continuity and momentum equations can, for incompressible flows without body forces, be written in tensor notation in Cartesian coordinates as:

$$\frac{\partial(\rho\overline{u}_i)}{\partial x_i} = 0 \,, \tag{9.18}$$

$$\frac{\partial(\rho\overline{u}_i)}{\partial t} + \frac{\partial}{\partial x_j}\left(\rho\overline{u}_i\overline{u}_j + \rho\overline{u_i'u_j'}\right) = -\frac{\partial\overline{p}}{\partial x_i} + \frac{\partial\overline{\tau}_{ij}}{\partial x_j} \,, \tag{9.19}$$

where the $\overline{\tau}_{ij}$ are the mean viscous stress tensor components:

$$\overline{\tau}_{ij} = \mu\left(\frac{\partial\overline{u}_i}{\partial x_j} + \frac{\partial\overline{u}_j}{\partial x_i}\right) . \tag{9.20}$$

Finally the equation for the mean of a scalar quantity can be written:

$$\frac{\partial\rho\overline{\phi}}{\partial t} + \frac{\partial}{\partial x_j}\left(\rho\overline{u}_j\overline{\phi} + \rho\overline{u_j'\phi'}\right) = \frac{\partial}{\partial x_j}\left(\Gamma\frac{\partial\overline{\phi}}{\partial x_j}\right) . \tag{9.21}$$

The presence of the Reynolds stresses and turbulent scalar flux in the conservation equations means that the latter are not closed, that is to say, they contain more variables than there are equations. Closure requires that some approximations, which usually take the form of prescribing the Reynolds stress tensor and turbulent scalar fluxes in terms of the mean quantities.

It is possible to derive equations for the higher order correlations e.g., for the Reynolds stress tensor, but these contain still more unknown correlations that require modeling approximations. These equations will be introduced later but the important point is that it is impossible to derive a closed set of exact equations. The approximations introduced are called *turbulence models.*

9.4.2 Simple Turbulence Models and their Application

To close the equations we must introduce a turbulence model. To see what a reasonable model might be, we note, as we did in the preceding section, that in laminar flows, energy dissipation and transport of mass, momentum, and energy normal to the streamlines are mediated by the viscosity, so it is natural to assume that the effect of turbulence can be represented as an increased viscosity. This leads to the eddy viscosity model:

$$-\rho\overline{u_i'u_j'} = \mu_t\left(\frac{\partial\overline{u}_i}{\partial x_j} + \frac{\partial\overline{u}_j}{\partial x_i}\right) - \frac{2}{3}\rho\delta_{ij}k \,; \tag{9.22}$$

$$-\rho\overline{u_j'\phi'} = \Gamma_t\frac{\partial\overline{\phi}}{\partial x_j} \,. \tag{9.23}$$

In Eq. (9.22), k is the turbulent kinetic energy:

$$k = \frac{1}{2}\overline{u_i'u_i'} = \frac{1}{2}\left(\overline{u_x'u_x'} + \overline{u_y'u_y'} + \overline{u_z'u_z'}\right) . \tag{9.24}$$

The last term in Eq. (9.22) is required to guarantee that, when both sides of the equation are contracted (the two indices are set equal and summed over), equation remains correct. Although the eddy viscosity hypothesis is not correct in detail, it is easy to implement and, with careful application, can provide reasonably good results for many flows.

In the simplest description, turbulence can be characterized by two parameters: its kinetic energy, k, or a velocity, $q = \sqrt{2k}$, and a length scale, L. Dimensional analysis shows that:

$$\mu_t = C_\mu \rho q L \,, \tag{9.25}$$

where C_μ is a dimensionless constant whose value will be given later.

In the simplest practical models, mixing length models, k is determined from the mean velocity field using $q = L\,\partial u/\partial y$ and L is a prescribed function of the coordinates. Accurate prescription of L is possible for simple flows but not for separated or highly three-dimensional flows. Mixing length models can therefore be used only for relatively simple flows; they are also known as zero-equation models.

The difficulty in prescribing the turbulence quantities suggests the use of partial differential equations for their calculation. Since a velocity and a length scale are needed, a model based on two such equations is a logical choice. In almost all such models, an equation for the turbulent kinetic energy, k, determines the velocity scale. The exact equation for this quantity is not difficult to derive:

$$\begin{aligned}\frac{\partial(\rho k)}{\partial t} + \frac{\partial(\rho \overline{u}_j k)}{\partial x_j} &= \frac{\partial}{\partial x_j}\left(\mu \frac{\partial k}{\partial x_j}\right) - \frac{\partial}{\partial x_j}\left(\frac{\rho}{2}\overline{u'_j u'_i u'_i} + \overline{p' u'_j}\right) - \\ &\quad \rho \overline{u'_i u'_j}\frac{\partial \overline{u}_i}{\partial x_j} - \mu \overline{\frac{\partial u'_i}{\partial x_k}\frac{\partial u'_i}{\partial x_k}} \,.\end{aligned} \tag{9.26}$$

The terms on the left side of this equation and the first term on the right need no modeling. The last term represents the product of the density ρ and the dissipation, ε, for which we shall give an equation below. The second term on the right represents *turbulent diffusion* of kinetic energy and is modeled by a gradient diffusion assumption:

$$-\frac{\rho}{2}\overline{u'_j u'_i u'_i} + \overline{p' u'_j} \approx \frac{\mu_t}{\sigma_k}\frac{\partial k}{\partial x_j} \,, \tag{9.27}$$

where μ_t is the eddy viscosity defined above and σ_k is a *turbulent Prandtl number* whose value is approximately unity.

The third term of the right side of Eq. (9.26) represents the *rate of production* of turbulent kinetic energy by the mean flow, a transfer of kinetic energy from the mean flow to the turbulence. If we use the eddy viscosity hypothesis (9.22) to estimate the Reynolds stress, it can be written:

$$P_k = -\rho \overline{u'_i u'_j}\frac{\partial \overline{u}_i}{\partial x_j} \approx \mu_t \left(\frac{\partial \overline{u}_i}{\partial x_j} + \frac{\partial \overline{u}_j}{\partial x_i}\right)\frac{\partial \overline{u}_i}{\partial x_j} \tag{9.28}$$

and the development of the turbulent kinetic energy equation is complete.

The choice of the length scale equation is less obvious. The most popular model makes use of the fact that, in so-called equilibrium turbulent flows,

i.e., ones in which the rates of production and destruction of turbulence are in near-balance, the dissipation, ε, and k and L are related by:

$$\varepsilon \approx \frac{k^{3/2}}{L} \,. \tag{9.29}$$

This allows one to use an equation for the dissipation as a means of obtaining both ε and L. No constant is used in Eq. (9.29) because the constant can be combined with others in the complete model. A number of other *two-equation* models have been proposed; the interested reader is referred to the book by Wilcox (1993).

Although an exact equation for the dissipation can be derived from the Navier-Stokes equations, the modeling is so severe that it is best to regard the entire equation as a model. We shall therefore make no attempt to derive it. In its most usual form, this equation is:

$$\frac{\partial(\rho\varepsilon)}{\partial t} + \frac{\partial(\rho u_j \varepsilon)}{\partial x_j} = C_{\varepsilon 1} P_k \frac{\varepsilon}{k} - \rho C_{\varepsilon 2}\frac{\varepsilon^2}{k} + \frac{\partial}{\partial x_j}\left(\frac{\mu_t}{\sigma_\varepsilon}\frac{\partial \varepsilon}{\partial x_j}\right) \,. \tag{9.30}$$

In this model, the eddy viscosity is expressed as:

$$\mu_t = \rho C_\mu \sqrt{k} L = \rho C_\mu \frac{k^2}{\varepsilon} \,. \tag{9.31}$$

The model based on Eqs. (9.26) and (9.30) is called the $k-\varepsilon$ model and has been widely used. This model contains five parameters; the most commonly used values are:

$$C_\mu = 0.09; \quad C_{\varepsilon 1} = 1.44; \quad C_{\varepsilon 2} = 1.92; \quad \sigma_k = 1.0; \quad \sigma_\varepsilon = 1.3 \,. \tag{9.32}$$

The implementation of this model is relatively simple. The RANS equations have the same form as the laminar equations provided the molecular viscosity, μ, is replaced by the effective viscosity $\mu_{\text{eff}} = \mu + \mu_t$. The most important difference is that two new partial differential equations need to be solved. This would cause no problem but, because the time scales associated with the turbulence are much shorter than those connected with the mean flow, the equations for the $k - \varepsilon$ model (and essentially any other turbulence model) are much stiffer than the laminar equations. Thus, there is little difficulty in the discretization of these equations other than one to be discussed below but the solution method has to take the stiffness into account.

For this reason, in the numerical solution procedure, one first performs an outer iteration of the momentum and pressure correction equations in which the value of the eddy viscosity is based on the values of k and ε at the end of the preceding iteration. After this has been completed, an outer iteration of the turbulent kinetic energy and dissipation equations is made. Since these equations are highly nonlinear, they have to be linearized prior to iteration. After completing an iteration of the turbulence model equations, we are ready to recalculate the eddy viscosity and start a new outer iteration.

The stiffness is the reason why the mean flow and turbulence equations are treated separately in the method just described; coupling the equations would make convergence very difficult to obtain. Too large a time step (or its equivalent in an iterative method) can lead to negative values of either k of ε and numerical instability. It is therefore necessary to use under-relaxation in the iterative method for these quantities; the values are similar to the ones used for the momentum equations (0.6-0.8).

The profiles of the turbulent kinetic energy and its dissipation are typically much more peaked than the mean velocity profile. These peaks are difficult to capture; one should probably use a finer grid for the turbulence quantities than for the mean flow but this is rarely done. If the same grid is used for all quantities, there is a chance that the solution may contain wiggles which can, in turn, lead to negative values of the turbulence quantities locally. This possibility can be avoided by locally blending the central difference scheme with a low order upwind discretizations for the convective terms in the k and ε equations. This, of course, increases the error in the solution for these quantities but is necessary if the same gird is used for all quantities.

Boundary conditions are needed for the model equations. These are generally similar to the conditions applied to any scalar equation. However, at solid walls there may be significant differences. One possibility is to solve the equations accurately right up to the wall. Then the conditions to be applied are the standard no-slip ones for the velocity. In the $k-\varepsilon$ model, it is appropriate to set $k = 0$ at the wall but the dissipation is not zero there; instead one can use the conditions:

$$\frac{\partial \varepsilon}{\partial n} = 0 \quad \text{or} \quad \varepsilon = \mu \left(\frac{\partial \overline{v}_t}{\partial n} \right)^2 , \tag{9.33}$$

where v_t is the velocity component tangential to the wall, see Sect. 8.10, and n is the coordinate normal to wall. When this is done, it is generally necessary to modify the model itself near the wall. It is argued that the effects that need to be modeled are due to the low Reynolds number of the turbulence near the wall and a number of low Reynolds number modifications of the $k-\varepsilon$ model were proposed; see Patel et al. (1985) and Wilcox (1993) for a review of some of these modifications.

At high Reynolds number, the viscous sublayer of a boundary layer is so thin that it is difficult to use enough grid points to resolve it. This problem can be avoided by using *wall functions*, which rely on the existence of a logarithmic region in the velocity profile; the velocity profile of a turbulent boundary layer is shown in Fig. 9.9. In the logarithmic layer, the profile is:

$$u^+ = \frac{\overline{v}_t}{u_\tau} = \frac{1}{\kappa} \ln n^+ + B , \tag{9.34}$$

where $\overline{v}_t$ is the mean velocity parallel to the wall, u_τ is the shear velocity, $u_\tau = \sqrt{\tau_w/\rho}$, τ_w is the shear stress at the wall, κ is the so-called von Karman

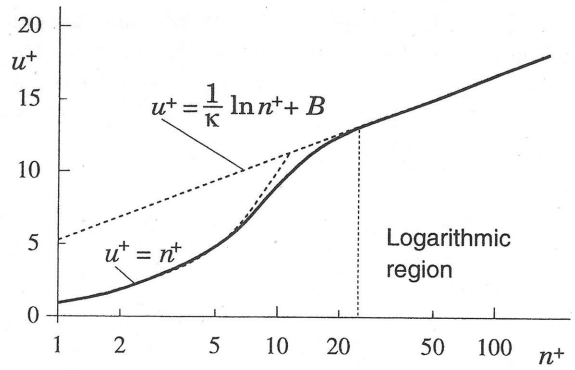

Fig. 9.9. The turbulent boundary layer: velocity profile as a function of distance normal to the wall (dashed lines are from corresponding equations, solid line represents experimental data)

constant ($\kappa = 0.41$), B is an empirical constant related to the thickness of the viscous sublayer ($B \approx 5.2$ in a flat plate boundary layer) and n^+ is the dimensionless distance from the wall:

$$n^+ = \frac{\rho u_\tau n}{\mu} . \tag{9.35}$$

It is often assumed that the flow is in local equilibrium, meaning the production and dissipation are nearly equal. If this is the case, one can show:

$$u_\tau = C_\mu^{1/4} \sqrt{k} . \tag{9.36}$$

From this equation and Eq. (9.34) we can derive an expression connecting the velocity at the first grid point above the wall and the wall shear stress:

$$\tau_w = \rho u_\tau^2 = \rho C_\mu^{1/4} \sqrt{k} \frac{\overline{v}_t}{\kappa \ln(n^+ E)} , \tag{9.37}$$

where $E = e^{\kappa B}$. The control volume nearest the wall has one face that lies on the wall. In the equation for the momentum parallel to the wall for that control volume, the shear stress at the wall is required. It may be taken from Eq. (9.37) i.e. the boundary condition is used to obtain a closed set of equations.

When these 'law of the wall' type boundary conditions are used, the diffusive flux of k through the wall is usually taken to be zero, yielding the boundary condition that the normal derivative of k is zero.

The dissipation boundary condition is derived by assuming equilibrium i.e. balance of production and dissipation in the near wall region. The production in wall region is computed from:

$$P_k \approx \tau_w \frac{\partial \overline{v}_t}{\partial n} , \tag{9.38}$$

which is an approximation to the dominant term of Eq. (9.28) that is valid near the wall; it is valid because the shear stress is nearly constant in this region. We need the dissipation (= production) at the midpoint of the control volume closest to the wall. The velocity derivative required can be derived from the logarithmic velocity profile (9.34):

$$\left(\frac{\partial \overline{v}_t}{\partial n}\right)_{\mathrm{P}} = \frac{u_\tau}{\kappa n_{\mathrm{P}}} = \frac{C_\mu^{1/4}\sqrt{k_{\mathrm{P}}}}{\kappa n_{\mathrm{P}}} , \tag{9.39}$$

which, together with Eq. (9.37), provides a second equation relating the wall shear stress and the velocity at the first grid point. From these two equations, both quantities may be computed.

When the above approximations are used, the equation for ε is not applied in the control volume next to the wall; instead, ε is at the CV center set equal to:

$$\varepsilon_{\mathrm{P}} = \frac{C_\mu^{3/4} k_{\mathrm{P}}^{3/2}}{\kappa n_{\mathrm{P}}} . \tag{9.40}$$

This expression is derived from Eq. (9.29) using the approximation for the length scale

$$L = \frac{\kappa}{C_\mu^{3/4}} n \approx 2.5\, n , \tag{9.41}$$

which is valid near wall under the conditions used to derive the 'law of the wall' model.

It should be noted that the above boundary conditions are valid when the first grid point is within the logarithmic region, i.e. when $n_{\mathrm{P}}^+ > 30$. Problems arise in separated flows; within the recirculation region and, especially, in the separation and reattachment regions, the above conditions are not satisfied. Usually the fact that wall functions are not valid in these regions is ignored and they are applied everywhere. However, if the above conditions are violated over a large portion of wall boundaries, serious modeling errors result. Low Reynolds number versions of the models should be used in such regions but their accuracy for a wide range of flows has not yet been demonstrated.

At computational boundaries far from walls, the following boundary conditions can be used:

– If the surrounding flow is turbulent:

$$\overline{u}\frac{\partial k}{\partial x} = -\varepsilon \;\; ; \;\; \overline{u}\frac{\partial \varepsilon}{\partial x} = -C_{\varepsilon 2}\frac{\varepsilon^2}{k} \tag{9.42}$$

– In a free stream:

$$k \approx 0 \;\; ; \;\; \varepsilon \approx 0 \;\; ; \;\; \mu_{\mathrm{t}} = C_\mu \rho \frac{k^2}{\varepsilon} \approx 0 . \tag{9.43}$$

At the inflow, k and ε are often not known; if they are available, the known values should, of course, be used. If k is not known, it is usually taken to have some small value, say $10^{-4}\,\overline{u}^2$. The value of ε should be selected so that the length scale derived from Eq. (9.29) is approximately one-tenth of the width of a shear layer or the domain size. If the Reynolds stresses and mean velocities are measured at inlet, ε can be estimated using the assumption of local equilibrium; this leads to (in a cross-section x = const.):

$$\varepsilon \approx -\overline{uv}\frac{\partial \overline{u}}{\partial y} . \tag{9.44}$$

A example of the application of the $k-\varepsilon$ model is given below.

9.4.3 Example: Flow Around a Valve

We briefly present an application of the $k-\varepsilon$ model. Valves in internal combustion engines are usually optimized by performing experiments on steady flows at several valve lifts. Lilek et al. (1991) reported the results of a combined numerical and experimental investigation of one particular geometry. The geometry was axisymmetric, so a 2D solution method using a boundary-fitted grid was used. Second-order CDS discretization and three systematically refined grids were used; the finest had 216 × 64 CVs. By comparing the solutions on these three grids, the discretization error was estimated to be 3% on the finest grid. Figure 9.10 shows portion of the second level grid.

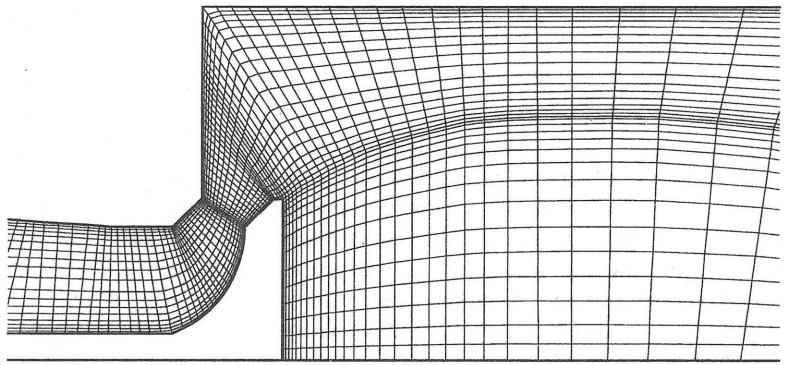

Fig. 9.10. Section of a grid (level two) used to calculate flow around a valve (from Lilek et al., 1991)

The computations were done before the experimental data was available; only the mass flow rate was prescribed. The inlet boundary was upstream of the valve, where the profiles for fully-developed annular flow (calculated separately for the same mass flow rate) were imposed. This is typical for a case

in which the exact conditions at the inlet are not known. The outlet boundary was placed in the exhaust pipe, one diameter downstream of the constriction, see Fig. 9.11. Zero streamwise gradient of all variables was specified there. At the walls, the wall functions described in the preceding sections were used.

The calculated streamlines and contours of the turbulent kinetic energy are shown in Fig. 9.11. A small separation at the valve throat is seen; major recirculation regions are found behind the valve and in the corner. The high-speed flow around the valve forms an expanding annular jet which hits the cylinder wall and flows along it toward the exit. High turbulence is created at the edges of this jet and along walls.

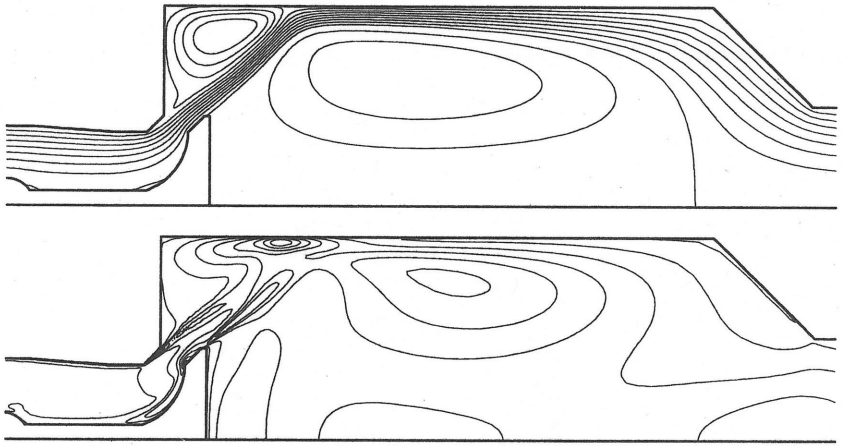

Fig. 9.11. Calculated streamlines (above) and contours of the kinetic energy (below) in flow around valve (from Lilek et al., 1991)

In Fig. 9.12 a comparison of calculated and measured axial and radial mean velocity profiles is shown. The profiles have rather complex shape, which is fairly well predicted; significant discrepancies between measurement and computation exist in some cross-sections and are probably due to the inadequacy of the model although this is not definitively established.

The important question is: can such calculations be used for optimization in engineering practice? The answer is yes, if care is taken. The authors were told that, in a study conducted by one car maker, the valve seat geometry found optimum by calculations using the method described above was also found best in an experimental study conducted independently.

Similar conclusions were drawn by Bertram and Jansen (1994), who used one commercial CFD code employing the $k-\varepsilon$ turbulence model and wall functions to calculate drag of three variants of a ship model. They found that the computed drag coefficient was low by about 12%; however, the relative

increase or reduction of the drag when the geometry was changed was predicted with the accuracy of about 2%. The best hull form from the numerical study was also the best in the towing tank.

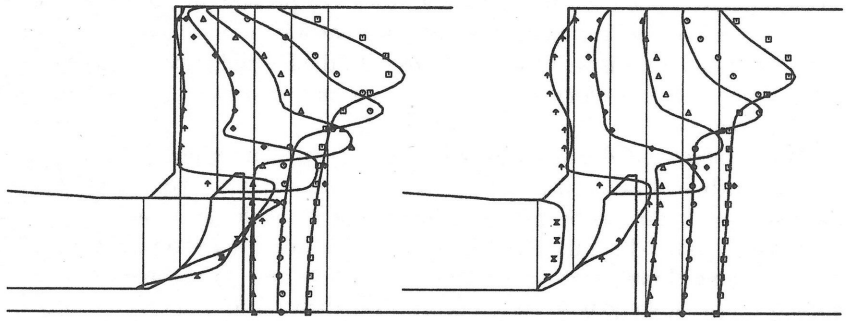

Fig. 9.12. Comparison of calculated and measured axial (left) and radial (right) velocity profiles in flow around valve (from Lilek et al., 1991)

A word of caution is necessary. New phenomena may appear in the flow when the geometry is changed and may not be well represented by the turbulence model. In such a case, computed results may not produce accurate answers. An example is provided by a modification of the above example; Lilek et al. (1991) reported poor agreement between predicted and measured velocity profiles downstream of the valve for halved lift.

9.5 Reynolds Stress Models

Eddy viscosity models have significant deficiencies; some are consequences of Eq. (9.22) not being valid. In three-dimensional flows, the Reynolds stress and the strain rate may not be related in such a simple way. This means that the eddy viscosity may no longer be a scalar; both measurements and simulations show that it becomes a tensor quantity. Anisotropic (tensor) models based on using the k and ε equations have been proposed. They are relatively new and untested so we shall not present them here; see Craft et al. (1995) for an example.

The most complex models in common use today are Reynolds stress models which are based on dynamic equations for the Reynolds stress tensor itself. These equations can be derived from the Navier-Stokes equations and are quite complicated. They contain triple correlations of the velocity fluctuations (e.g., $\overline{u_i' u_j' u_k'}$) as well as correlations of the velocity components and the pressure (e.g., $\overline{u_i' p'}$). These require modeling which can become rather complicated. For this reason, we shall not describe or discuss these models here.

The interested reader is referred to Launder (1989, 1990), Hanjalić (1994), Launder and Li (1994) and Craft and Launder (1995).

In three dimensions, these models require the solution of seven partial differential equations in addition to the equations for the mean flow. Still more equations are needed when scalar quantities are present in the flow. These equations are solved in a manner similar to that for the $k-\varepsilon$ equations. The only additional issue is that the equations with the Reynolds stress models are even stiffer than those for the $k-\varepsilon$ equations and even more care is required in their solution.

While there is no doubt that these models have a larger potential to represent the turbulent flow features more correctly that the two-equation models, their success so far has been moderate. Excellent results have been obtained for some flows in which the $k-\varepsilon$ type of models are known to perform badly (e.g., swirling flows, flows with strong curvature and with separation from curved surfaces, etc.); however, in some flows their performance was not better at all. A lot of research is going on in this field, and new models are often being proposed. Which model is best for which kind of flows (none is expected to be good for all flows) is not yet quite clear, partly due to the fact that in many attempts to answer this question numerical errors played a too important role so clear conclusions were not possible (Bradshaw et al., 1994). In most workshops held so far on the subject of evaluation of turbulence models, the differences between solutions produced by different authors using supposedly the same model were as large if not larger than the differences between the results of the same author using different models. This is one of the reasons why numerical accuracy is emphasized in this book; its importance can not be overemphasized.